Technical University of Denmark

DTU

Load Consequences when Sweeping Blades - A Case Study of a 5 MW Pitch Controlled Wind Turbine

Verelst, David Robert; Larsen, Torben J.

Publication date:
2010

Document Version
Publisher's PDF, also known as Version of record

DTU Library
Technical Information Center of Denmark

Load Consequences when Sweeping Blades - A Case Study of a 5 MW Pitch Controlled Wind Turbine

David R.S. Verelst, Torben J. Larsen
Risø-R-1724(EN)
August 2010

Author: David R.S. Verelst, Torben J. Larsen
Title: Load Consequences when Sweeping Blades - A Case Study of a 5 MW Pitch Controlled Wind Turbine
Division: Wind Energy Division

Abstract (max. 2000 char.):

The generic 5 MW NREL wind turbine model is used in Risø's aeroelastic simulator HAWC2 to investigate 120 different swept blade configurations (forward and backward sweep). Sensitivity for 2 different controllers is considered as well. Backward sweep results in a pitch to feather torsional moment of the blade, effectively reducing blade twist angles under increased loading. This behaviour results in decreased flap-wise fatigue and extreme loads, an increase for edge-wise fatigue loading and status quo or slight decrease in extreme loads (depending on the controller). Tower base and shaft-end bending moments are reduced as well. Forward sweep leads to an increase in angle of attack under loading. For a pitch controlled turbine this leads to an increase in fatigue and extreme loading in all cases. An controller inflicted instability is present for the more extreme forward swept cases. Due to the shape of considered sweep curves, an inherent and significant increase in torsional blade root bending moment is noted. A boomerang shaped sweep curve is proposed to counteract this problematic increased loading. Controller sensitivity shows that adding sweep affects some loadings differently. Power output is reduced for backward sweep since the blade twist is optimized as a rigid structure, ignoring the torsional deformations which for a swept blade can be significant.

Contents

1   Introduction

For the UPWIND project, the NREL 5 MW reference wind turbine model is used to investigate the influence of different blade sweep curves. It is expected that a swept blade planform can have a positive effect on load reduction due to the geometrical coupling between blade flapping and torsional deflections. An increased aerodynamic loading will cause the blade to twist to feather (reducing the angle of attack) or to stall (increasing angle of attack) as a result of this coupling effect. A sudden change in wind speed results in change in blade torsional loading, which affects the blade twist locally. The blade twist will have a faster response when compared to a classic pitch system. As a result, load fluctuations and hence fatigue loading can be reduced. Previous studies regarding swept wind turbine blades for pitch controlled turbines have indicated that a flap-wise fatigue load reduction can be observed for backward sweep (pitch to feather) [4] [5] [1]. Forward sweep will have a pitching to stall moment, causing larger angles of attack. For pitch controlled turbines, this leads to higher lift forces, hence the increase in fatigue and extreme loads. For stalled controlled blades, an increased angle of attack will lead to lower lift forces but likely increased drag, if the blade is operating at angles of attack larger than the stall angle.

For this investigation, Risø's aeroelastic wind turbine simulator HAWC2 [3] is used to explore 120 different sweep curves, for a 4-26 m/s wind speed range with fixed turbulence intensity (=0.18). The consequences for blade root fatigue and extreme loads are investigated (in non-pitching coordinates). A reduced pitch activity might be beneficial from a reliability point of view, therefore the travelled pitch angles are also considered, in order to quantify a change in pitch behaviour. Tower base and shaft-end loadings are briefly considered as well.

A controller sensitivity analysis is included for all sweep variants. Two different implementations of the controller as described in [2] are used: the original one provided by NREL (same version as provided with the FAST model of the 5 MW reference turbine) and an implementation done by Risø.

Simulation results from HAWC2 indicate that flap-wise fatigue and extreme loads can be decreased up to 10 and 15% respectively for a backward swept blade. For the same cases there is a penalty on edge-wise fatigue loads up to 7% and edge-wise extreme loads are increased up to 6% for the Risø controller and decreased up to 6% for the NREL controller. Travelled pitch angles are decreased when combining backward sweep and the Risø controller (up to 10%). For the NREL controller, an increase in pitch activity is noted (up to 8%). However, for those cases the NREL controller displays travelled pitch angles which are 10% lower with respect to the Risø controller results. Tower base fatigue and extreme loadings note reductions in the 10-15% range. Shaft torsional loadings are hardly affected, while extreme loadings for shaft tilting moments are reduced up to 25%. Further, shaft yaw and tilt fatigue loads reduce around 10-15% for backwards swept blades.

2 NREL 5 MW HAWC2 model

The generic 5 MW wind turbine designed by NREL [2] is used for this investigation. It is an 'open' design and the specifications are available in the mentioned report. The NREL 5 MW wind turbine is originally modelled in FAST, but is translated to an HAWC2 model at Risø. It is assumed that the HAWC2 model is in agreement with the FAST model since the given system eigenmodes have matching eigenfrequencies (FAST eigenfrequencies as given in [2]).

The FAST model is provided with a GH Bladed-style collective pitch controller, which is discussed in [2]. A Risø interpretation of this controller is available as well. Both controllers are used and compared in this report. Note that HAWC2 has a different DLL controller interface compared to FAST-Bladed. Some patches (a Bladed-to-HAWC2 interface) provide the necessary adjustments to match input and output streams correctly in this case.

Some key parameters of the NREL 5 MW machine are displayed in table 1. Modelling parameters and settings for HAWC2 are displayed in table 2.

The original aerodynamic coefficients are not changed for this investigation. In HAWC2, the radial component of the flow is not taken into account to calculate the lift forces, so the swept wing correction (as mentioned in [4]) is not required here. However, it is expected that the 3D aerodynamics of a swept blade are different when compared to unswept blades. The increased radial flow component might affect, among others, the 3D stall characteristics of the blade. It is considered beyond the scope of this report to elaborate further on the aerodynamic behaviour of swept blades.

NREL 5-MW reference turbine (HAWC2 model)	
Rating	5 MW
Rotor orientation, configuration	Upwind, 3 Blades
Control	Variable speed, Collective pitch
Drivetrain	High speed, Multiple-stage gearbox
Rotor, Hub diameter	126 m, 3 m
Hub height	90 m
Cut-in, Rated, Cut-out wind speed	3 m/s, 11.4 m/s, 25 m/s
Cut-in, Rated rotor speed	6.9 rpm, 12.1 rpm
Rated tip speed	80 m/s
Overhang, Shaft tilt, Precone	5 m, 0 deg, 0 deg
Rotor mass	110,000 kg
Nacelle mass	240,000 kg
Tower mass	347,460 kg

Table 1. Key parameters for the NREL 5 MW wind turbine

Dynamic stall	Stig Øye
Tower shadow	potential flow
Wind shear	none
Turbulence model	Mann
Turbulence intensity	for all wind speeds: 0.18

Table 2. HAWC2 simulation settings

3 Sweep-parameter space

A brute force method, consisting out of 120 different swept blade variants, is chosen to investigate the effects of different sweep variants on blade loading. The sweep curve is modelled as a simple exponential curve:

$$x = a \left(\frac{z - z_0}{z_e - z_0} \right)^b \tag{1}$$

The sweeping is superimposed to the baseline half chord positions. Starting point of the sweep curve, z_0, is taken at 14.35 m blade length (excluding the hub), which corresponds to the blade radial position for which the torsional stiffness is much lower when compared to more inward sections (see figure 1).
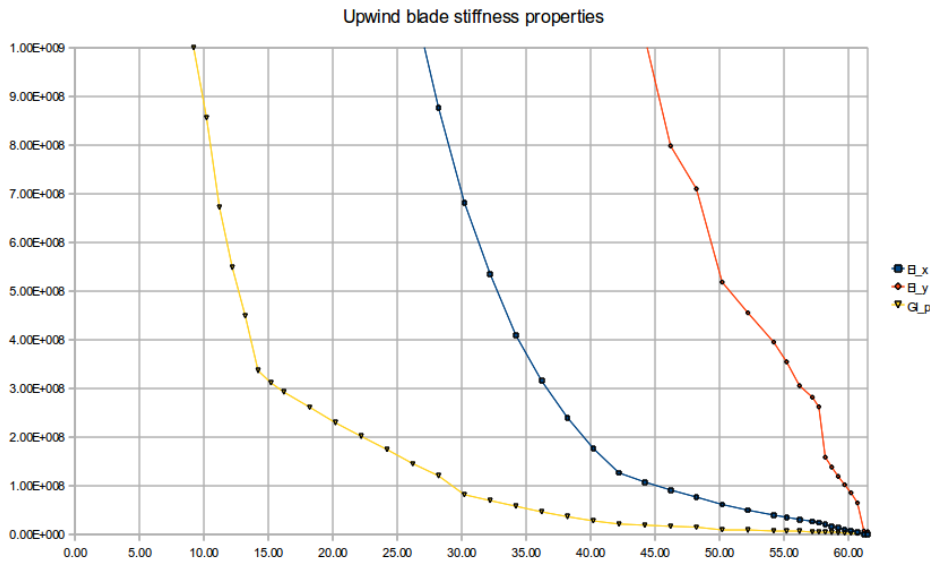

Figure 1. Blade spanwise stiffness distribution

In [7] it was noted that some of the sweep curves investigated produced a high twisting moment at the inner more torsional stiff blade stations, resulting in higher loads relatively to lower induced twist angles. Since a comprehensive structural design study is not considered for this report, it is assumed that a good starting point for the sweep curve is at 14.35 m blade radial length (excluding hub). For a=1 (a tip offset of 1 m), the 5 different curve exponents are plotted in the figure 2 (note that x and y axes do not have the same scale).
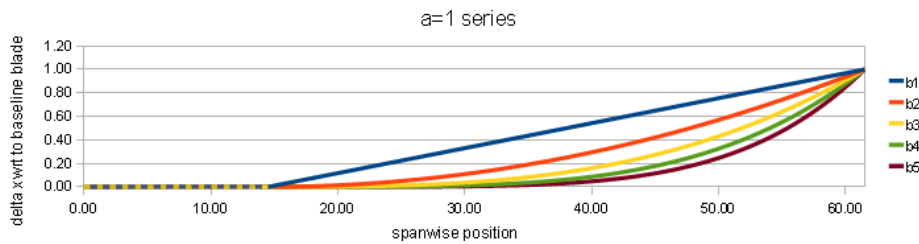

Figure 2. Different swept blade planforms

24 different values for the tip offset, ranging from -6 m (backward sweep) to 6 m (forward sweep) with a step size of 0.5 m, combined with 5 sweep exponents (1, 2, 3, 4 and 5) results in 121 different blade variants (including the original unswept configuration). The forward swept cases will introduce a pitch to stall moment (in blade torsion), the backward swept cases a pitch to feather moment. For each blade sweep configuration, turbulent wind speed from 4 m/s till 26 m/s are considered (10 minute series, all have fixed turbulence intensity of 0.18 and no wind shear). As a result, 1452 turbulent HAWC2 simulations are set-up for each controller. Additionally, for each of the 121 blade variants, a single simulation is run for a deterministic wind speed (without wind shear), covering wind speed step changes of 1 m/s (from 4 to 26 m/s in 22.5 minutes). The total set of 3025 simulations required approximately 8 hours on one of Risø's Linux clusters (running HAWC2 in the MS Windows emulator Wine).

4 Results

4.1 Figure definitions

For the comparison of the data, the percentage difference with respect to (abbreviated as wrt) either the unswept blade variant or the NREL controller is used throughout this report, which is defined as:

$$\% \text{ difference} = \left(\frac{x_{sweep}}{x_{nosweep}} - 1 \right) * 100 \qquad \% \text{ difference} = \left(\frac{x_{\text{Risø}}}{x_{\text{NREL}}} - 1 \right) * 100$$

The sweep curve domain is represented on 2 axes: the exponent (b) on the horizontal axes and the tip-offset (a) (see equation 1) on the vertical axis. For the values of a=0 and/or b=0, the un-swept results are applicable.

Unless stated otherwise, all mentioned blade root bending moments refer to a non-pitching coordinate system.

4.2 Instabilities for forward sweep

From the flap-wise blade root fatigue loads for all sweep variants (see figure 3), a significant increase can be observed for the forward swept cases. This is caused by a pitch controller induced instability, as can be verified in figure 4, where step changes in wind speed for a deterministic wind field is simulated. Time series for the turbulent wind field are displayed in figure 5. It shows that the instability persists under turbulent conditions, for both the NREL and Risø implementations of the controller.
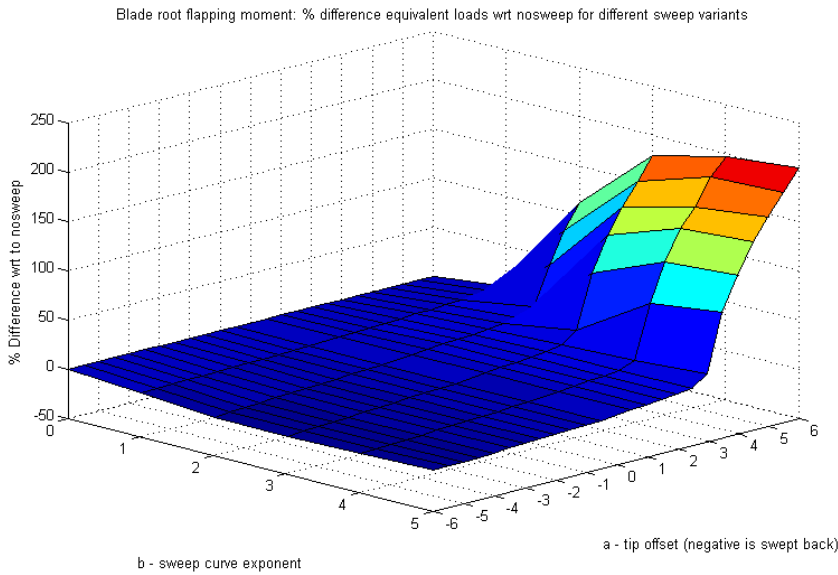

Figure 3. Flap-wise fatigue load, percentage difference with respect to unswept case, Risø controller. Note that for this and subsequent plots, b=0 (zero tip-offset) and a=0 (zero sweep curve exponent) corresponds to the unswept blade.

For the remainder of this report, we will focus on the sweep curves which are not troubled by these pitch induced instabilities, meaning the forward swept off-sets from 3.0 m till 6.0 m are ignored. This leaves a tip off-set range starting from -6.0 m (backwards) and ends at 2.5 m (forwards).
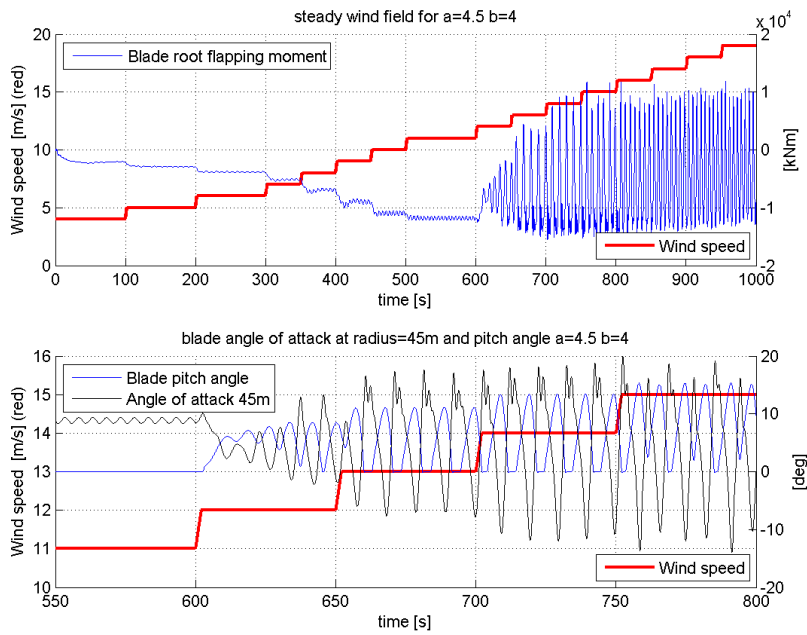
Figure 4. Pitch controller (Risø version) induced instabilities for a deterministic wind field: forward sweep. The top figure clearly shows an dramatic increase in the fluctuations of the flap-wise blade root bending moment. The figure below shows that pitch controller is out of phase with the angle of attack.
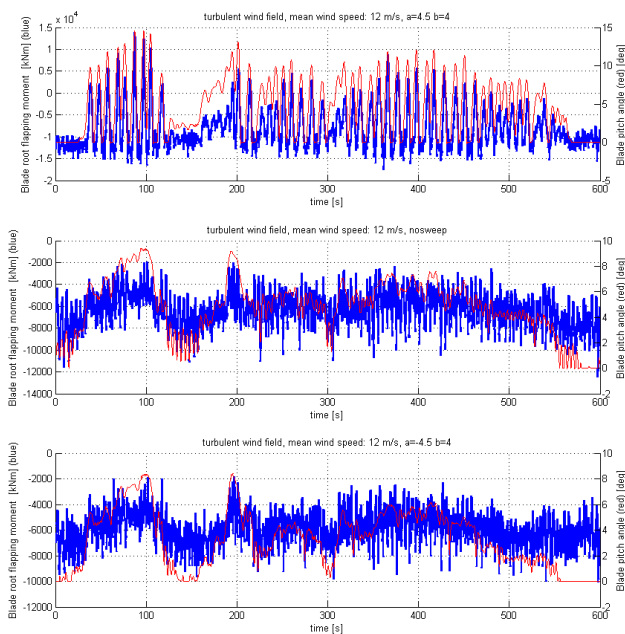

Figure 5. Comparing pitch controller (Risø version) behaviour and blade root bending moments for forward- (a=4.5), no- and backward sweep (a=-4.5) at 12 m/s average wind speed. NREL controller has a comparable behaviour (figure not shown here). Note that the forward sweep has very large load fluctuations, resulting in high positive values as well, while for no- and backward sweep in general a negative sign exists.

Risø–R–1724(EN)

4.3 Fatigue Calculations

Fatigue calculations have been performed for a Rayleigh probability wind speed distribution, as defined in the IEC standards for a class II wind turbine. Considered wind speeds ranged from 4 to 26 m/s, with a step size of 2 m/s. A rainflow counting algorithm available on the Matlab Central website [6] is used to determine the fatigue loads. Total wind turbine life time is set at 20 years. The fatigue loads for the blade root bending moments (non-pitching coordinates for flap-, edge-wise and torsion) are considered for this investigation and they are plotted in figures 6, 7 and 8.

Forward sweep (pitching towards stall) increases the fatigue load for all 3 blade root bending moments. Backward sweep however (pitch to feather), can decrease the fatigue loads of the flap-wise blade root bending moment up to 10%, while edge-wise fatigue loads will increase up to 2-6% for the same cases. Any sweep will dramatically affect torsional loading, with the fatigue load increasing up to 400%.

Results from the NREL controller shows comparable trends, although small differences are observed: flap-wise fatigue loads are within a 2% margin of the Risø controlled results, edge-wise a 3% margin and torsional a 5% margin.

In order to avoid these significant increased torsional fatigue loadings, a different blade planform could be used. When sweeping the inner part of the blade in the opposite direction with respect to the outward part, the torsional root moment is expected to be lowered. The result could be a boomerang shaped blade planform.
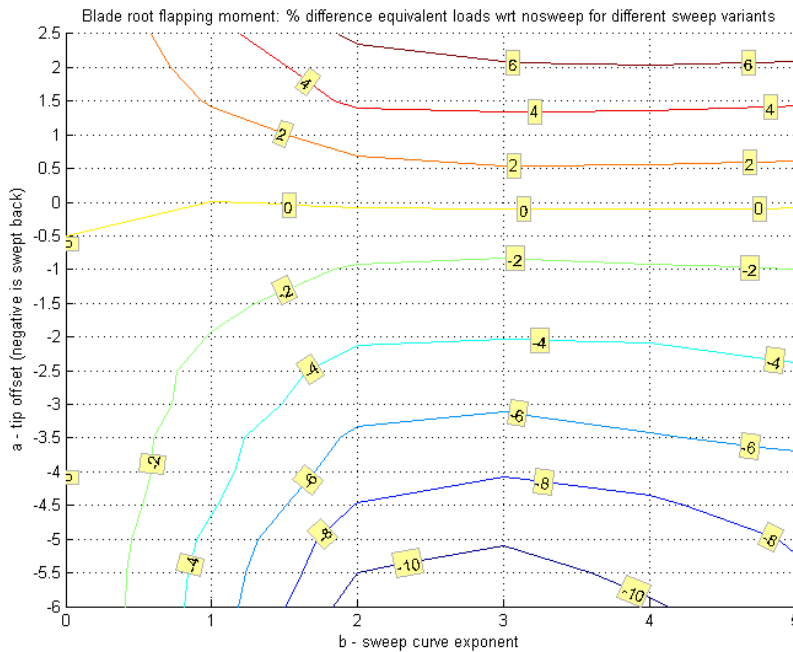

Figure 6. Flap-wise fatigue load, percentage difference with respect to unswept case, Risø controller. Note that for this and subsequent plots, b=0 (zero tip-offset) and a=0 (zero sweep curve exponent) corresponds to the unswept blade. The 10% flap-wise fatigue load reduction occurs for the most extreme values of the backward swept tip-offset, for 3 different sweep curves (2, 3 and 4)
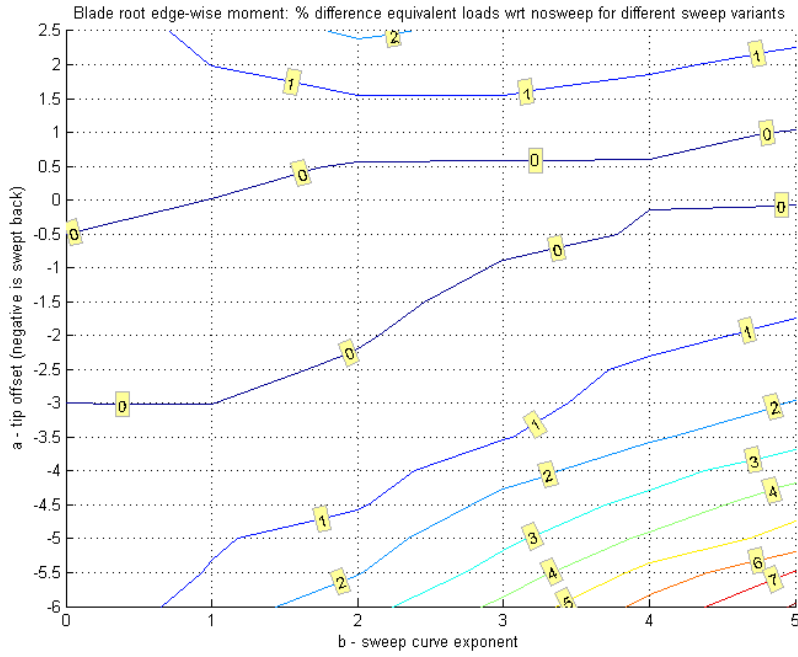
Figure 7. Edge-wise fatigue load, percentage difference with respect to unswept case, Risø controller. The sweep curves resulting in the most beneficial flap-wise reduction (a = -6, b = 2 to 4), have an increase in edge-wise fatigue loads of 2 to 6%.
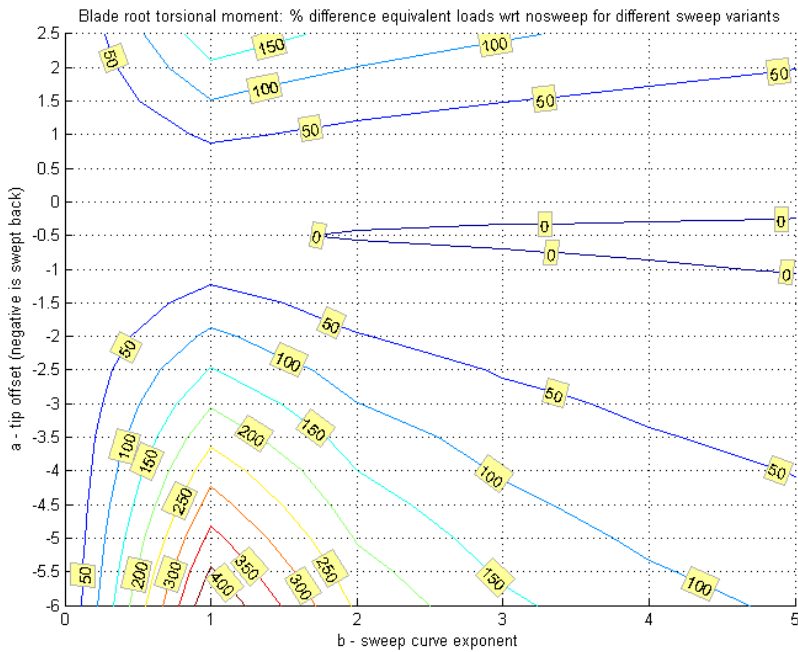

Figure 8. Torsional fatigue load, percentage difference with respect to unswept case, Risø controller. Inherent dramatic increase due to proposed sweep shape.

4.4 Extreme blade root bending moments

For each blade variant, the extreme blade root bending moments are gathered. Normally, an extreme load investigation would require simulations at multiple turbulent seed numbers. In this case only one seed number is considered. No load extrapolation methods are applied.

A somewhat different trend can be noticed for the extreme loads. The controller has larger influence on the results, although again for the flap-wise blade root bending moments a reduction of up to 15% can be obtained by sweeping the blades backwards (see figures 9 and 10).

The edge-wise extreme blade root bending moments show an increase of up to 8% for the most extreme sweep in combination with the Risø controller, while the NREL controller has a decrease of up to 6% for backward sweep (see figures 11 and 12).

Extreme torsional loads are increased significantly, due to the increased mean values. A general higher torsional loading is the result of this sweeping configuration (see figures 13 and 14).
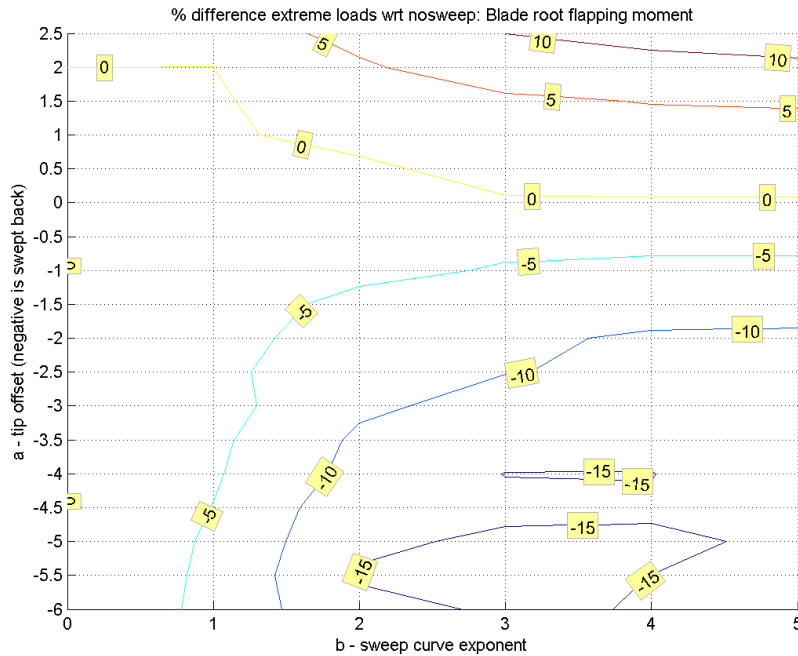

Figure 9. Percentage difference of extreme blade root flapping moments, Risø controller with respect to (wrt) no-sweep. The effect on the extreme loads is comparable to the reduction in fatigue loading: up to 15% reduction for the most backward swept cases.
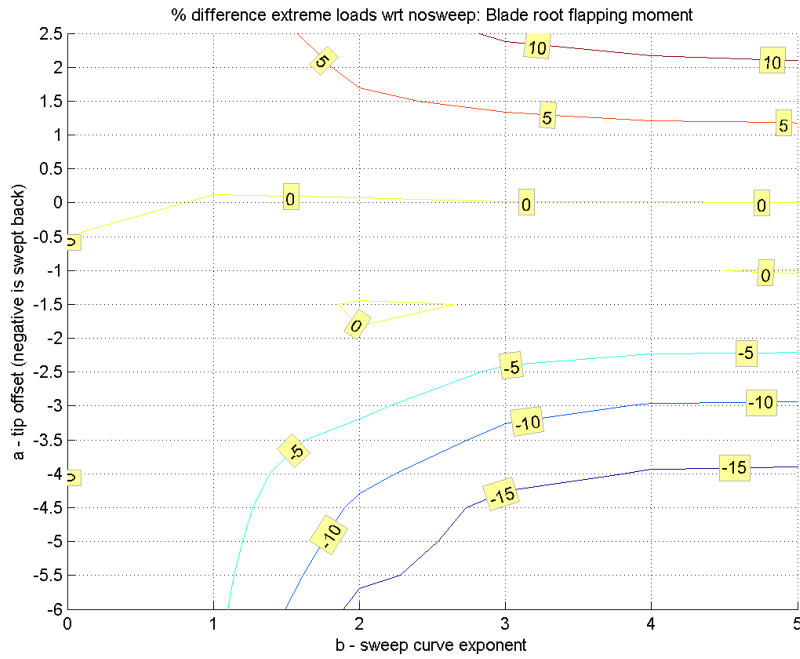
Figure 10. Percentage difference of extreme blade root flapping moments, NREL controller wrt no-sweep. The reduction follows the same trend compared to the fatigue load reduction.
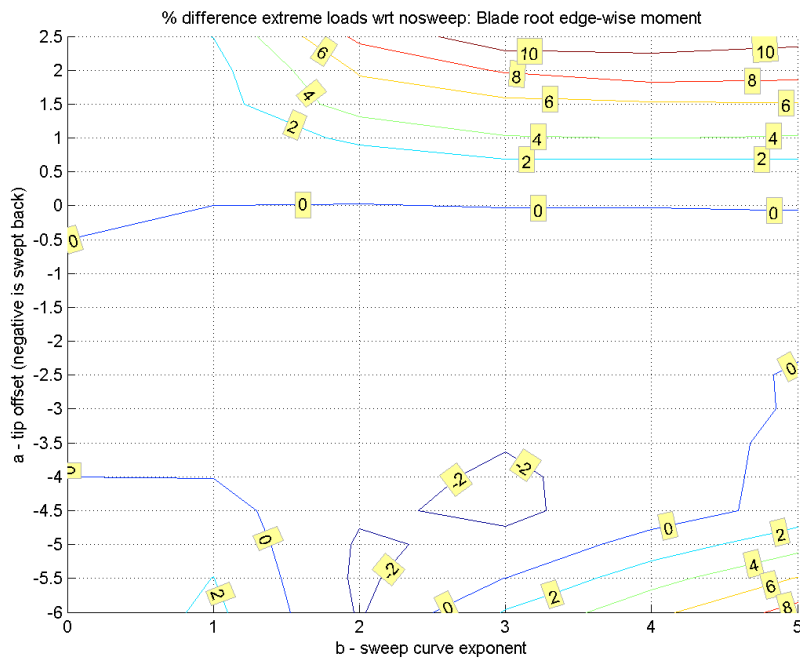

Figure 11. Percentage difference of extreme blade root edge-wise moments, Risø controller wrt no-sweep. The extreme load consequences for edge-wise bending moments are somewhat more beneficial when compared to the increase in fatigue loading (for the Risø controller). Only one backward swept case (the most 'extreme' sweep curve) results in an increase of around 8%, while some cases even show a decreased extreme load occurrence.
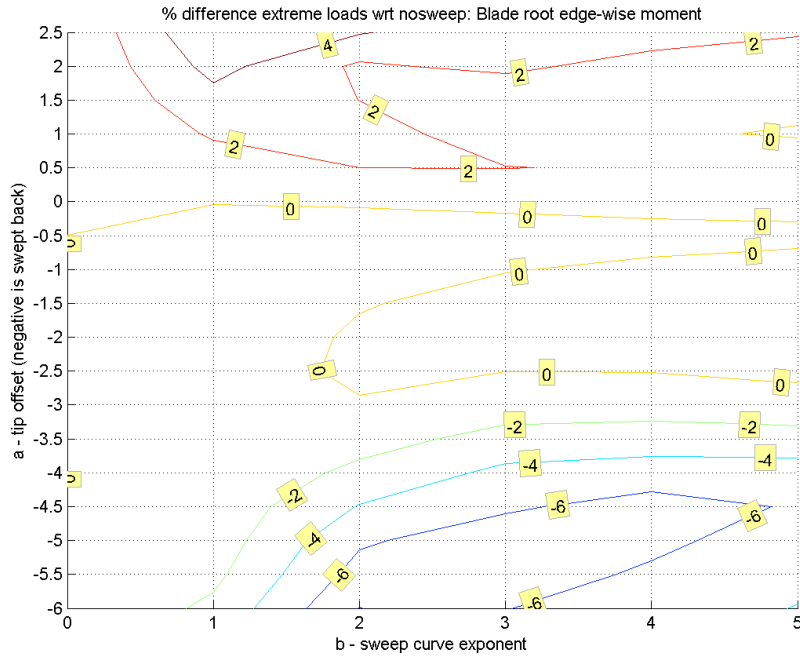
Figure 12. Percentage difference of extreme blade root edge-wise moments, NREL controller wrt no-sweep. In general lower values for the extreme loads, while fatigue loads had a slight increase.
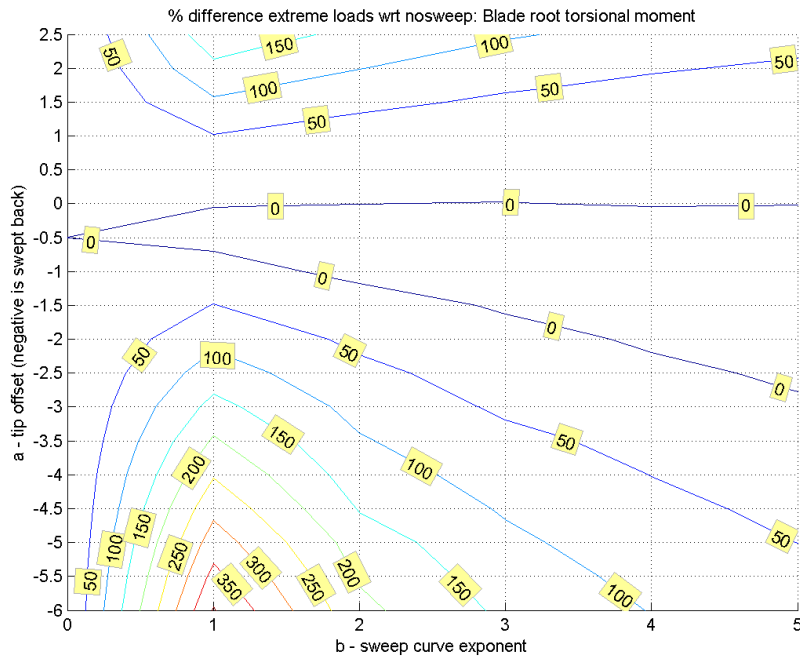

Figure 13. Percentage difference of extreme blade root torsional moments, Risø controller wrt no sweep. Same trend when compared to fatigue loading: the inherent and significant increase of the average torsional moment dominates the extremes as well.
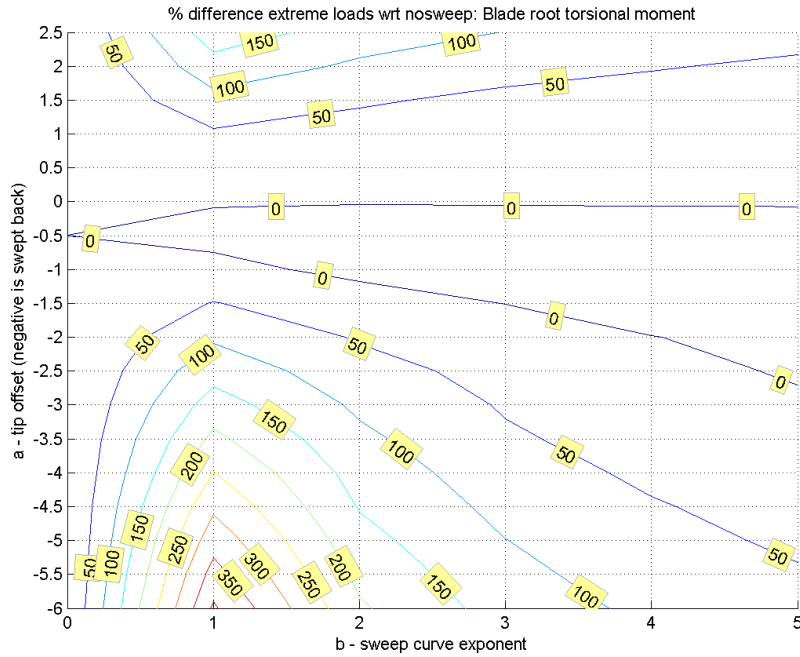
Figure 14. Percentage difference of extreme blade root torsional moments, NREL controller wrt no sweep. Same trend when compared to fatigue loading: the inherent and significant increase of the average torsional moment dominates the extremes as well.
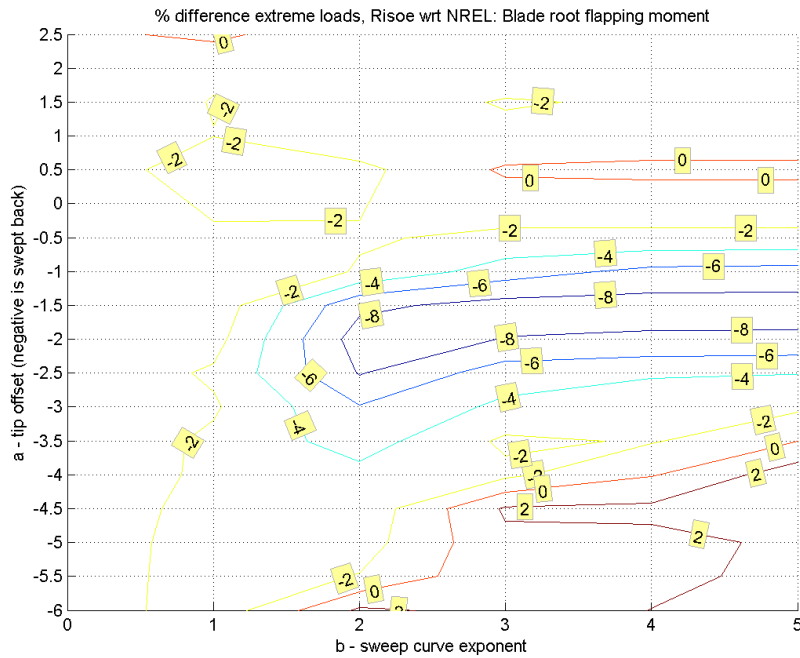

Figure 15. Percentage difference of extreme blade root flapping moments, Risø controller wrt NREL. For most cases the Risø controller results in lower extreme loads, while for the most extreme sweep curves, the NREL version performs slightly better.
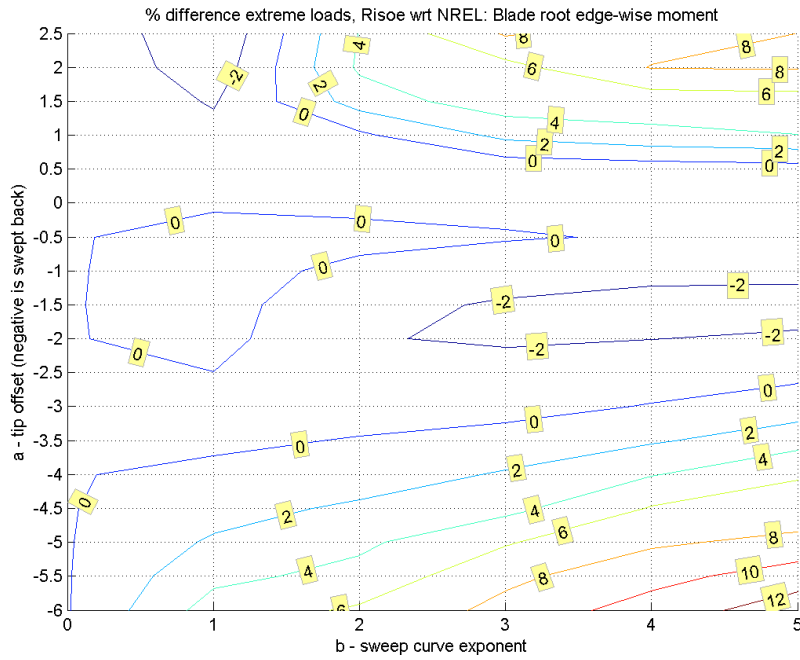
Figure 16. Percentage difference of extreme blade root edge-wise moments, Risø controller wrt NREL. For most cases the NREL controller has lower extreme loads, a reduction of up to 12% for the most extreme sweep curve
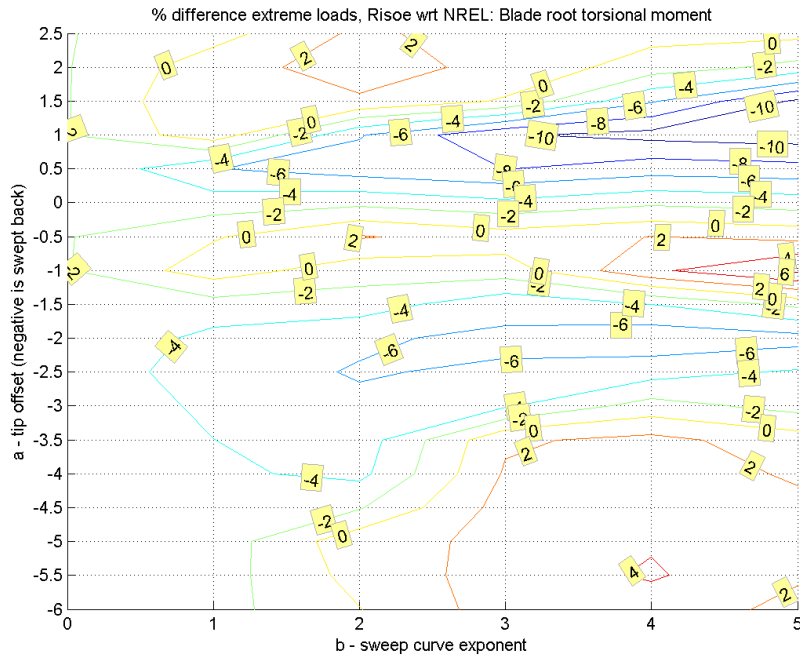

Figure 17. Percentage difference of extreme blade root torsional moments, Risø controller wrt NREL. Since the increase over the no-sweep variants is very large (up to 400%), the difference between both controllers seems insignificant (up to 10%).

4.5 Travelled pitch angle

An indication of the pitch behaviour can be given by evaluating the travelled pitch angle over its life time. A standard IEC Rayleigh wind speed distribution (same as used for the fatigue calculations) weights each wind speed when summing up the integration of pitching speed over time.

It is interesting to note that the two considered controllers have a different behaviour. The Risø controller will result in a reduced pitch activity over its lifetime for backward swept blades (wrt unswept case, see figure 18), since pitching will start at higher wind speeds due to the feathering of the loaded blade. The NREL controller shows a different trend (see figure 19): almost all sweep variants show a modest increase in pitch activity. However, note that the travelled pitch angles for the NREL controller are for all swept cases lower than for the Risø version (see figure 19).

These results indicate that in this case, comparable controllers perform different when blade sweep is added.

Figure 18. Percentage difference of the travelled pitch angle over its lifespan for the Risø controller with respect to the original un-swept blade. Adding sweep results in a 10% reduction. Note that for backward swept blade, the pitching will start at slightly higher wind speeds due to the torsional deformation of the blade (pitch to feather).
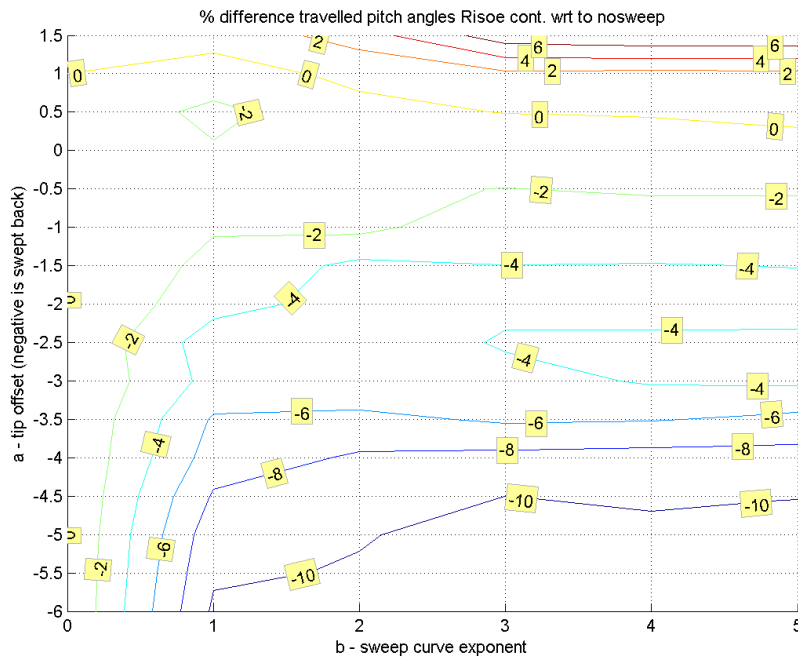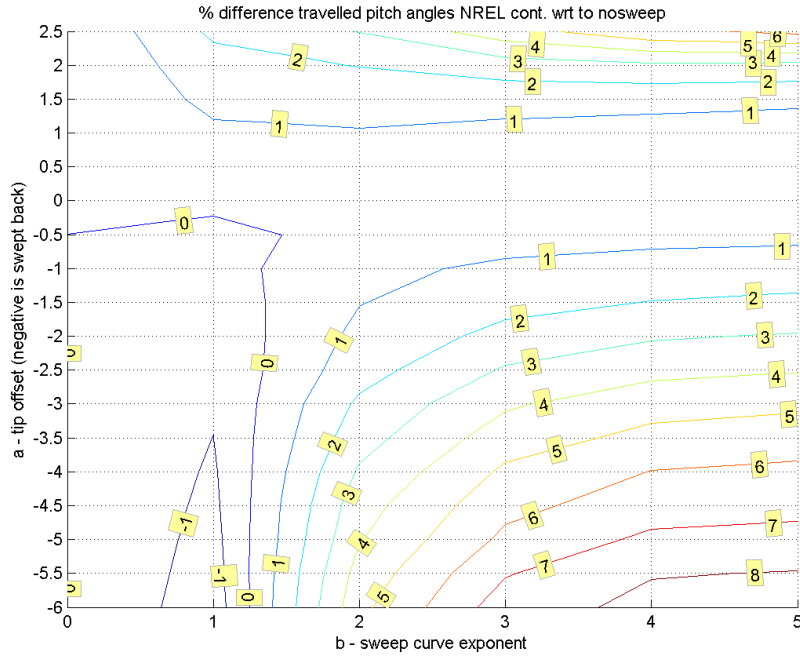
Figure 19. Percentage difference of the travelled pitch angle over its lifespan for the NREL controller with respect to the original un-swept blade. Adding sweep affects the NREL controller in a different way when compared to the Risø version: an increased pitch activity is noted.
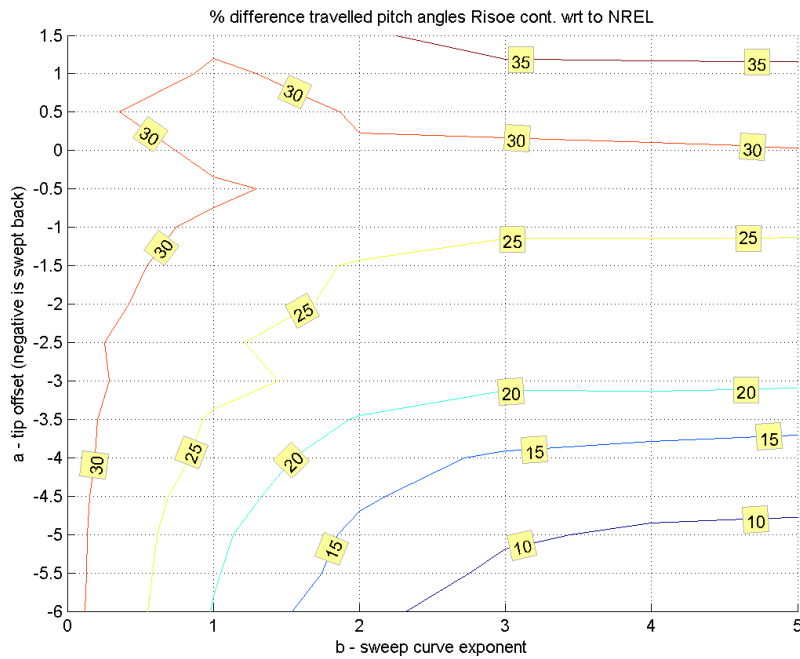

Figure 20. Percentage difference of the Risø controller over the NREL version for the travelled pitch angles over its lifespan. In general the NREL controller has a lower pitch activity when compared to the Risø controller. The difference is smaller for more backward swept blades.

4.6 Shaft and tower base loading

When briefly looking at the load consequences for tower base bending moments and shaft-rotor connection (shaft-end / main bearing), following observations are made:

- shaft-end tilting extreme and fatigue loading is decreased up to 10% for highly swept back blades (see figure 21)

- shaft-end torsional loading is hardly affected (for both fatigue and extreme loading)

- shaft-end yawing extreme moments decreases up to 25% (see figure 22) and up to 15% fatigue load reduction for highly swept backward blades

- tower base torsional, for-aft: fatigue and extreme loads show reductions in the order of 10% for backward swept blades

- tower base side-to-side fatigue loading shows a varied response: for some backward swept blades a slight increase, for others a decrease (-5 +5 % range, see figure 23), controller sensitivity is higher when compared to other tower base bending moment components. The extreme loads show a reduction (up to 10%), which is comparable to the for-aft and torsional reduction in fatigue loads.
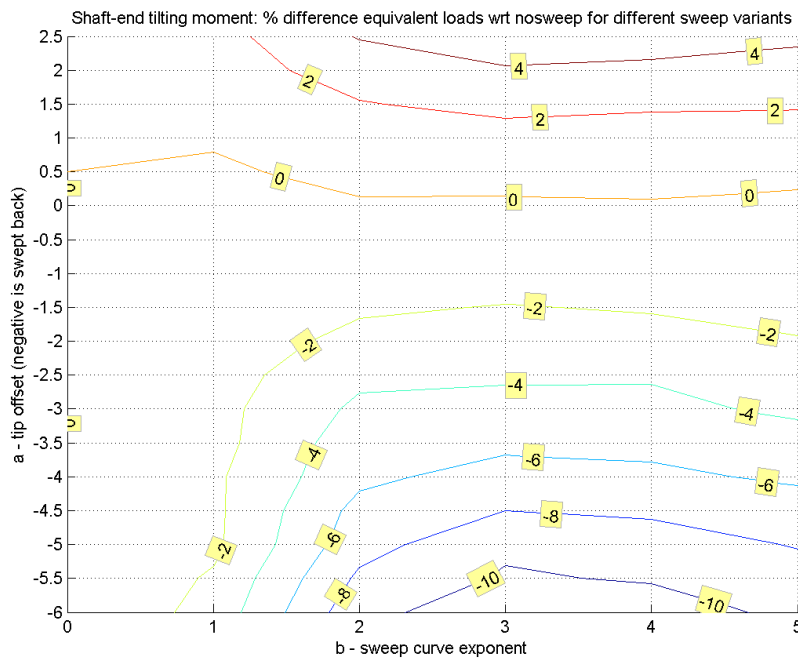

Figure 21. Percentage difference of shaft end (shaft-rotor connection) fatigue tilt-loading for the Risø controller with respect to the original un-swept blade. Comparable trends for the tilt-extreme loadings and NREL controller.
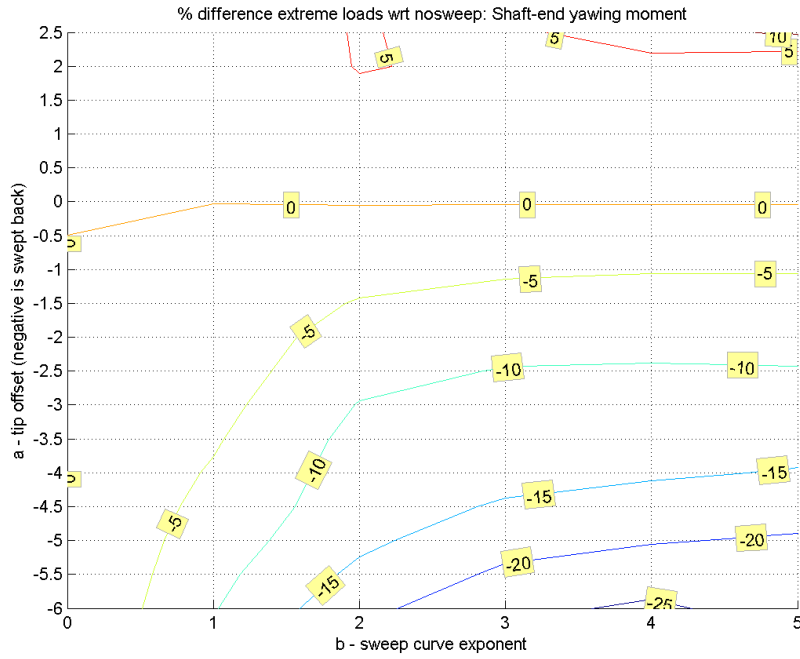
Figure 22. Percentage difference of shaft-end (shaft-rotor connection) extreme yaw-loading for the Risø controller with respect to the original un-swept blade. The most significant reductions of all considered loads in this report are noticed here (up to 25%).
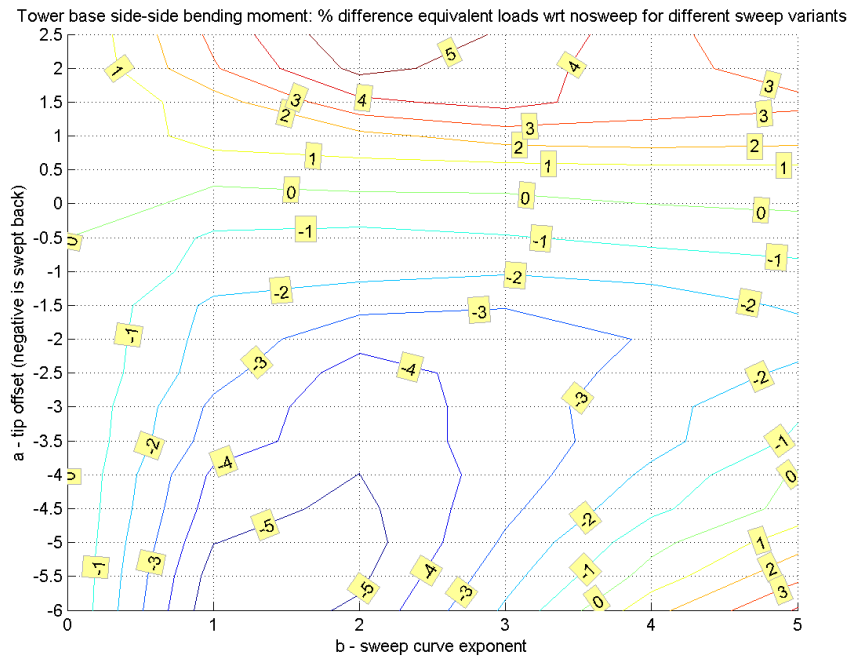

Figure 23. Percentage difference of tower-base side-to-side fatigue loading for the Risø controller with respect to the original un-swept blade. While the majority of the sweep curves results in decreased fatigue loads, the most extreme sweep curves cause an increase.

4.7   Power production

The torsional deformation of the blade has a consequence on the below rated power output, since the blade pre-twist distribution is not changed for this investigation. The backward swept blade will operate at lower angles of attack due to the pitching to feather torsional moment (see figure 25), as a result, power production is lower when compared to the original unswept blade (see figure 24). The geometrical and aerodynamic optimization for a swept blade should also take the torsional deformation of the blade into account.
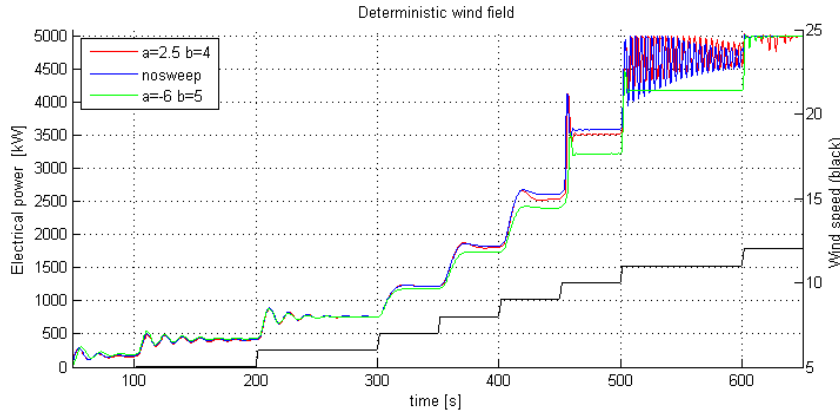
Figure 24. Electrical power output for deterministic wind speeds in below rated conditions (Risø controller). Wind speed on the right axis, electrical power on the left. For backward sweep (green line), it is clear that the power output is reduced.

Figure 25. Angle of attack for deterministic wind speeds (Risø controller), radial stations at 16% and 71% blade radius. Wind speed is displayed on the right axis, angle of attack on the left. Note that closer to the tip, the difference in angle of attack due to the increased torsional deformation of the blade is significant.

Conclusions

Backward sweep shows for both considered controllers lower blade root flap-wise fatigue (reduction up to 10%) and extreme loads (reduction up to 15%).
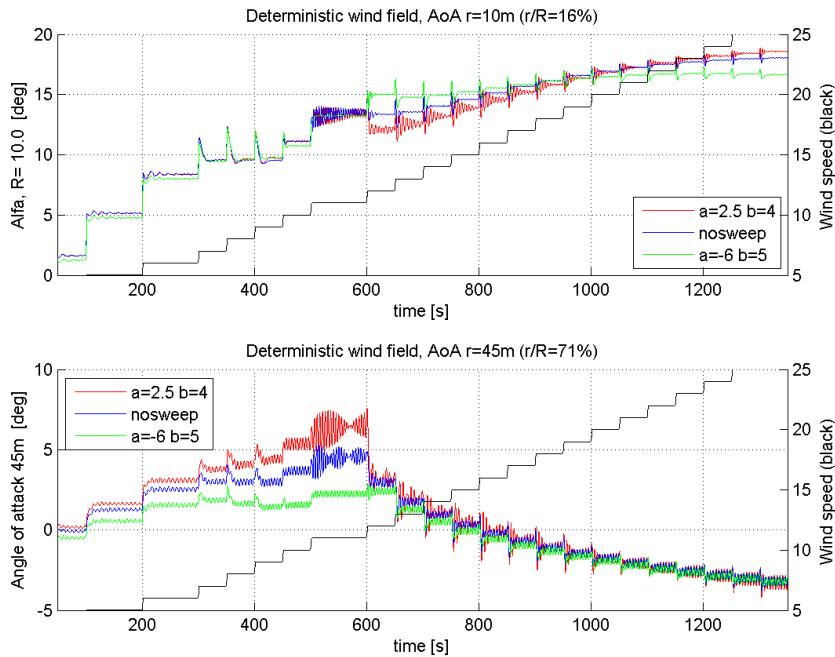
Edge-wise blade root fatigue loading is increased (up to 7%) for both controllers. The extreme loads are more dependent on the controller: the Risø implementation shows an increase for highly swept backward blades (up to 8%) and a status quo for most of the other swept-back curves, while the NREL controller noted a general decrease for backward sweep (up to 6%).

Blade root torsion is for fatigue and extreme loads severely affected under both controllers (up to 400%). Due the shape of the considered sweep geometries, this is an inherent penalty. A different sweep, like a boomerang-shaped blade, is suggested in order to reduce this unwanted side-affect.

Travelled pitch angles depend on the controller configuration. Adding sweep for the Risø controller let to a decreased pitch travel (up to 10%). The NREL controller increased the travelled pitch angles up to 8%. However, the NREL controller has a lower pitch activity in general (compared to Risø's version), where for less backward sweep the difference starts at 30%, but reduces to 10% for the most extreme backward sweep.

Due to the torsional deformation of the blade, the geometric pre-twist distribution is not any more the same as the initial (optimal) one. As a result, power output of backward swept blades is lower in below rated conditions. When sweeping the blade, the pre-twist distribution should be different when compared to the unswept blade. This process will require an geometrical-aerodynamic optimization routine which accounts for the structural induced twist angles under loading.

Backward sweep results in reduced loadings on shaft and tower as well. Shaft torsion is not affected significantly (changes in a ±1.5% range). Shaft yaw- and tilting moments are decreased up to 15% in fatigue loading and up to 25% in extreme loading. Tower torsional and for-aft base bending moments show reductions up to 10-15% for fatigue and extreme loadings. Tower side-to-side base bending moments show both a modest in- and decrease in fatigue loading while extreme loadings are reduced in general (up to 10%).

Forward sweep will result in all cases in increased fatigue and extreme loads. Travelled pitch angles are increased as well. Both controllers displayed unstable behaviour for the highly forward swept configurations.

| Load consequences backward sweep wrt no-sweep | | | | | Risø | |
| Controller | Risø | | NREL | | wrt NREL | |
Loads	fat.	ext.	fat.	ext.	fat.	ext.
Blade root flap	-8 %	-15 %	-10 %	-15 %	0 %	+2 %
Blade root edge	+7 %	+6 %	+3 %	-4 %	+3 %	+12 %
Blade root torsion	+50 %	+50 %	+50 %	+50 %	+1 %	+2 %
Tower base FA	-3 %	-8 %	-3 %	-4 %	na	-3 %
Tower base SS	+2 %	-12 %	+4 %	-6 %	na	-10 %
Tow. base torsion	-10 %	-15 %	-8 %	-15 %	na	-2 %
Shaft-end tilt	-10 %	-2 %	10 %	-10 %	na	+20 %
Shaft-end yaw	-15 %	-20 %	-14 %	-20 %	na	-3 %
Shaft-end torsion	+ 1.5 %	0.5 %	+ 1.0 %	-2.5 %	na	+1.5 %
Travelled pitch	-10 %		+8 %		+10 %	

Table 3. Overview of approximate load consequences for a pitched controlled, extreme swept wind turbine

References

[1] Thomas Ashwill, Gary Kanaby, Kevin Jackson, and Michael Zuteck, *Sweep-Twist adaptive rotor (STAR) blade development*, 2010.

[2] J. Jonkman, S. Butterfield, W. Musial, and G. Scott, *Definition of a 5-MW reference wind turbine for offshore system development*, Tech. Report NREL/TP-500-38060, National Renewable Energy Laboratory (NREL), February 2009.

[3] Torben J. Larsen, *HAWC2 user manual*, Tech. Report Ris-R-1597(ver. 3-9)(EN), Ris National Laboratory, Denmark, September 2009.

[4] S. Larwood, M. Zuteck, U. C. Davis, and M. D. Z. Consulting, *Swept wind turbine blade aeroelastic modeling for loads and dynamic behavior*, AWEA Windpower (2006), 117.

[5] S. M Larwood, *Dynamic analysis tool development for advanced geometry wind turbine blades*, PhD, University of California, 2009.

[6] Adam Nieslony, *MATLAB central - rainflow counting algorithm*, http://www.mathworks.com/matlabcentral/fileexchange/3026-rainflow-counting-algorithm, 2010.

[7] M. Zuteck, *Adaptive blade concept assessment: curved planform induced twist investigation*, Tech. Report SAND2002-2996, Sandia National Laboratories, October 2002.

Risø DTU is the National Laboratory for Sustainable Energy. Our research focuses on development of energy technologies and systems with minimal effect on climate, and contributes to innovation, education and policy. Risø has large experimental facilities and interdisciplinary research environments, and includes the national centre for nuclear technologies.